Lasers in Manufacturing Conference 2019

Time-resolved pump-probe microscopy of ultrashort laser pulse irradiated bulk aluminum and stainless steel

Jan Winter[a,b,c], Stephan Rapp[a,b,c], Cormac McDonnell[a], Maximilian Spellauge[a], Michael Schmidt[b], Heinz P. Huber[a*]

[a]*Lasercenter, Department of Applied Sciences and Mechatronics, Munich University of Applied Sciences, Lothstrasse 34, 80335 Munich, Germany*
[b]*Lehrstuhl für Photonische Technologien, Friedrich- Alexander-Universität Erlangen-Nürnberg, Konrad-Zuse-Strasse 3-5, 91052 Erlangen, Germany*
[c]*Erlangen Graduate School in Advanced Optical Technologies (SAOT), Friedrich-Alexander-Universität Erlangen-Nürnberg, Paul-Gordan-Straße 6, 91052 Erlangen, Germany*

Abstract

Metals irradiated with ultrashort laser pulses pass through a sequence of physical processes over a wide range of timescales, from femtoseconds to microseconds. Especially, the relaxation of the photomechanical material removal, known as spallation, has not been well investigated experimentally on this timescale. In this article, the complete timescales for the processes involved in ablation of industrially relevant metals, Al and the stainless steel alloy (AISI304), are analyzed and visualized, from the initial pulse absorption to the material removal occurring on a microsecond time scale. These results advance our understanding of a key aspect of the laser–material interaction pathway and can lead to optimization of associated applications ranging from material processing to laser surgery.

Keywords: ultrashort pulses, pump-probe microscopy, ablation dynamic, metals, aluminium, stainless steel, femtosecond ablation

1. Introduction

Ultrashort pulse lasers have become increasingly important for material processing during the last decades [1, 2]. One decisive feature of ultrafast laser processing is that heat diffusion to surrounding regions of the

*Corresponding author. Tel.: 089-1265-1686; fax: 089-1265-1603
E-mail address: Heinz.huber@hm.edu

processed area is reduced [3]. In consequence, such laser sources allow for e.g. the surface micro- and nanostructuring [4, 5], the micromachining [6, 7] or the hole drilling [8–10] with high precision and process speed. Recently, micromaching of metals was demonstrated using ultrashort laser double pulses with pico- to nanosecond time delay [11, 12] or burst sequences of several tens of nanosecond duration [13, 14]. Significant influence on the ablation rate was observed in dependency on the pulse delay and the pulse number. Thus, the interaction of subsequent pulses is strongly dependent on the transient material properties which are influenced by the irradiation with the first pulse of the sequence.

When an ultrashort laser pulse irradiates the surface of a metallic sample under stress-confinement, high pressure is created in the irradiated volume because the ultrafast heating occurs faster than the expansion of the heated material can take place [21, 22]. A pressure wave followed by a rarefaction wave is emitted into the material [23]. The rarefaction wave induces the removal of molten material by a spallation process just above the threshold fluence for ablation – in this case only a thin molten layer is ablated – or by a phase explosion at higher fluences [24]. The material motion and bulging occurs on a pico- and nanosecond timescale and the actual material disintegration and ablation after several tens of nanoseconds up to microseconds.

Even though lot of theoretical work was published [23, 24], experimental studies of the material behavior during and after the pulse impact are necessary to test the theories and to identify the processes that influence the laser- matter-interaction of subsequent pulses. Pump-probe techniques with ultrahigh temporal resolution are well suited for such investigations. Hohlfeld et al. published pump-probe reflectometry measurements to study electron and lattice dynamics in laser irradiated gold and nickel in the first picoseconds after the pump-pulse impact [25]. Additionally, the technique was applied to study the bulging of laser irradiated aluminum [26] and gold [27, 28] taking place on a timescale of up to about 10 ns. Domke et al., who investigated the laser-induced removal of thin molybdenum films [29], published first studies of the complete ablation process from the femto- to microsecond regime. Later, a scattered-light pump-probe setup was applied to explore the morphological surface structure formation on laser irradiated zone on a time span up to several hundreds of nanoseconds [30].

In this paper, the ablation process of the industrially relevant metals aluminum and stainless steel is investigated on a time span ranging from the pulse impact up to delay times of 10 µs when the ablation process is in its final state. For this, a pump-probe reflectometry measurement method was applied.

2. Material and Methods

2.1. Used samples

Ultrapure aluminum (> 99.999 %) and and stainless steel AISI304 was used as sample material. To avoid thin film effects, substrate material with a thickness of 500 µm was chosen. To guarantee a homogeneous sample surface quality for the pump-probe measurements the samples were carefully polished to an average surface finish of Ra < 25 nm.

2.2. Pump-probe microscopy setup

Pump-probe reflectometer (PPR) setups include a Nd:glass laser (Spectra Physics, “femtoRegen”) emitting pump-pulses at a center wavelength of λ_{pump} =1056 nm and a pulse duration of τ_{pump} = 680 fs. To obtain probe-pulses at a center wavelength of λ_{probe} =528 nm and a pulse duration of τ_{probe} = 540 fs, the laser pulses are frequency doubled in a second harmonic generation module. The PPR allows the ablation process

observation by measuring time- and space-resolved relative reflectivity changes of the laser irradiated material. The temporal observation interval ranges from the pump-pulse impact up to the final ablation state after 10 µs. For this, the PPR combines an optical delay line and an electronically triggered actively q-switched probe-laser (InnoLas, "picoloAOT", λ_{picolo} = 532 nm, τ_{picolo} = 600 ps).

The optical delay line enables the data collection up to delay time of 4 ns with a temporal resolution of about 540 fs defined by τ_{probe}. The electronically triggered laser enables the observation of advanced delay times with a temporal resolution of 600 ps. A detailed description of the measurement procedure and the data post processing is described in [31].

The measurement were performed at fluence proportional to the related ablation threshold fluence F_{thr}. The ablation threshold fluence was determined by the D^2-method [32]. The threshold ablation fluences F_{thr} for Al and stainless steel are determined to 0.42 J/cm^2 and 0.22 J/cm^2 for the p-polarized pump pulse with the pulse duration of 680 fs at central wavelength of λ_{pump}=1056 nm at an incident angle of 35°.

3. Results

3.1. First delay time range from 0 ps to 40 ps

In figure 1 time-resolved PPR data of laser irradiated Al and stainless steel are displayed up to a delay time of 40 ps.

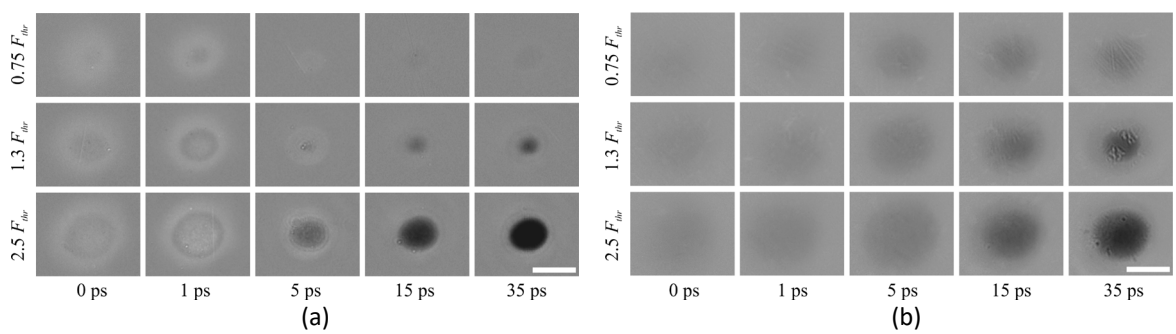

Fig. 1. PPR data of Al in (a) and stainless steel AISI304 in (b) are shown for three different applied flunces. White bar = 30 µm

In the corresponding PPR images of Al and stainless steel a continuous decrease of the relative reflectivity from pump pulse impact up to 40 ps can be observed. At delay time of 0 ps the pump pulse energy is absorbed by free electrons in conduction band [15] and electrons are thermally excited to higher energy levels. In stainless steel, this electronic excitation corresponds to a redistribution of occupied electronic states around the Fermi edge leading to decrease of reflectivity [34], as shown in Fig.1 (a) and (b) as black areas. In the following time delays up to 40 ps the optical response of stainless steel is overlapped with the influence of surface expansion and the rarefaction of the surface and cannot be separated in the optical signal of reflectivity. Whereas, in Al it is assumed that no electronic contribution in the optical response takes place and the rapid drop in reflectivity after 1 ps can mainly be attributed to the optical material response, which is influenced by the lattice heating and thus by an ultrafast rarefaction of the heated liquid material.

The rarefaction of the surface induces an early material motion of the surface [33]. Here, a continuous decrease of reflectivity in Al can be observed in the first 40 ps after the pump-pulse impact affected by continues surface expansion.

3.2. Second delay time range from 100 ps to 1 ns

In this section the material motion is analyzed on a timescale between 100 ps and 1 ns. For this, only the ablation processes at the fluence of 2.5 F_{thr} are considered because the effects are the most pronounced here. At the fluence of 1.3 Fthr the material shows qualitatively the same behavior but at a smaller spatial scale and at the fluence of 0.75 F_{thr} no ablation occurs.

The PPR images showing the material motion are displayed in figure 2 for applied fluence of 2.5 F_{thr}. In Al and stainless steel the material response is slightly different. After the initial reflectivity decrease down to the corresponding reflectivity changes of $\Delta R/R = -0.3$ (Al) and $\Delta R/R = -0.85$ (AISI304) up to delay times Δt = 50 ps, the reflectivity in the spot center increases again and shows an optical visible oscillating behavior in the following up to delay times of Δt = 1 ns. In Fig. 2, these oscillations become visible as ring structures in the laser irradiated area. These so called Newton rings were already observed in a variety of metals (Al, Ti, Au) during the ablation process at fluences just above the threshold fluence for ablation [26]. They can be explained by light interference from light reflected at a curved and a flat surface. The curved surface is formed during the ablation process by the creation of an about 20 nm thin partly transparent film that delaminates from the substrate and bulges with increasing process duration. The flat surface is given by the underlying substrate. This ablation of a thin liquid film is referred to the "spallation process" [24]. The bulging height *h* of the spallation film can be estimated from the experimental data in Fig. 2 by the simple interference formula $h = m \lambda/(2n)$. Therein, *m* is the interference order, λ the probe wavelength of pulse and *n* the refractive index of the medium between spallation film and substrate. In this estimation, this medium is assumed to be vacuum with n = 1. With m = 2.5 for Al and 3.5 for stainless steel at a delay time of 500 ps bulging velocities of v_{Al} = 1650 m/s and v_{Steel} = 1850 m/s are obtained.

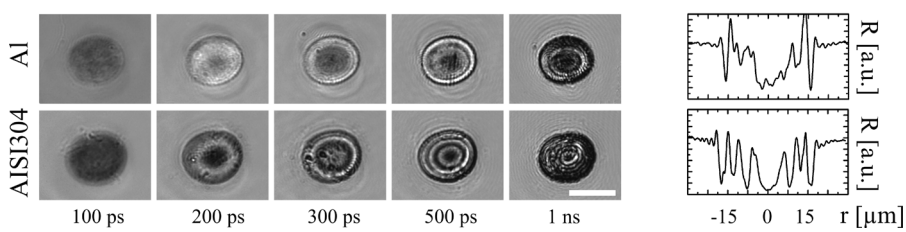

Fig. 2. PPR images of laser irradiated Al and stainless steel AISI304 at a pulse peak fluence of 2.5 Fthr for delay times between 100 ps and 1 ns. Right: Cross sections of the reflectivity for each material at a delay time of 500 ps. White bar = 30 µm

3.3. Final delay time range from 2.5 ns to 10 µs

In this section, the actual ablation process is analyzed. For this, PPR images continuing the PPR sequences from Fig. 2 are displayed at the top of Fig. 3 on a timescale between 2.5 ns and 10 µs. In the laser irradiated areas in Al and stainless steel display a reduced reflectivity (Al: $\Delta R/R = -0.9$ and stainless steel: $\Delta R/R = -0.5$) at the delay time of 2.5 ns. The number of Newton rings becomes too high (> m= 7) and thus their spatial distance too small (< 2 µm) to be resolved individually. For the investigated metals the reflectivity in the spot center stays decreased up to a delay time of about 10 ns and starts then to slowly increase (at 100 ps: $\Delta R/R = -0.8$ (Al) and -0.3 (AISI304)) due the particle ejection and thus the reflectivity is increasing up to the value of the initial surface is reached.

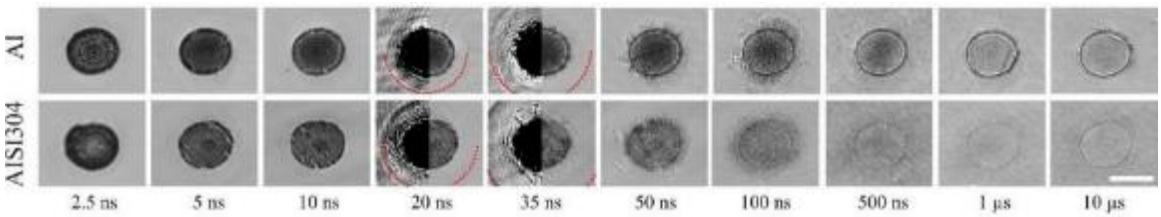

Fig. 3. PPR images of laser irradiated Cu, Al and stainless steel AISI304 at a pulse peak fluence of 2.5 Fthr for delay times between 2.5 ns and 10 µs. Selected images with enhanced contrast are shown on the left half. Red dotted lines mark the shock wave front. White bar = 30 µm.

The results shown in Figure 3 give a visualization of the nanoparticle/cluster dynamics in Al and stainless steel metals from 2.5 ns to 10 µs. The PPR visual images results show clear nanoparticle/cluster ejection at times from 50-100 ns. An estimation of the overall nanoparticle ejection times can be given by examining the recovery of the reflectivity of the probe pulse to the steady time reflectivity. During the time scales where nanoparticle ejection is taking place, significant attenuation of the probe pulse will take place. Finally, the recovery of the reflectivity takes place for Al and AISI304 on time scales of 100 ns to 2 µs and from 100 ns to 1 µs indicating the end of significant particle ejection and the achieved final state.

3.4. Influence of pulse separation time on laser ablation efficiency

Various studies have been performed on the ablation efficiency with the meaning of an energy specific ablation volume of double pulses, pulse bursts and different repetition rates. Summarizing these mainly three temporal efficiency regimes become clear which can be compared to the delay times of the study at hand. In the first delay time range from 0 ps to 40 ps the efficiency exhibits a maximum for zero delay times, which drops to about 50% within about 10 ps [35, 36]. Secondly a time interval between about 100 ps to 10 ns was revealed, in which the efficiency is further deceased and remaining below 50% [35]. And thirdly, the final time interval up from about 10 ns to the final state in the µs-range, where the efficiency is gradually recovering to the original maximum value of 100%. When the PPR results here are compared to the state of the art, following consequences can be speculated: in the first interval a subsequent pulse can “weaken” the stress confinement and by that lower efficiency, in the second interval the interaction with the spallation layer can push down efficiency below 50% and in final interval the thinning particle cloud can restoring efficiency at 100% again in the µs range.

To hold efficiency high the interaction with the propagating ablation products should be avoided over all three delay time intervals. A subsequent pulse will have an optimum effect, when the complete process has reached a steady-state and finished in the µs time range corresponding to repetition rates in the order of MHz.

3.5. Influence of pulse duration ablation efficiency

In recent years it has been demonstrated that the pulse duration has an effect on the energy specific ablation volume, or in short ablation efficiency: the efficiency is dropping from about 100% at 500 fs pulse duration to about 50% at 10 ps and is reduced to even less than 50% in the so called “valley of tears” up to about pulse durations of 10 ns [38]. The study at hand demonstrates that the ablation process in steel and Al (or more general in industrial metals) initiated with a sub-ps pulse exhibits a pronounced photo-mechanical

character, which is driven by the pressure build up due to the energy deposition and is indicated by the ultrafast drop of material density within a few ps (see section 3.1).

To hold ablation efficiency high, the temporal energy deposition should be faster than the mechanical reaction of the material. Optimally this is achieved for pulse durations less than a few ps.

4. Summary and conclusion

In this study the complete visualization and quantification of the dynamic optical properties and material motion were analyzed for industrially relevant metals, namely aluminum and stainless steel.
Overall the ablation dynamics of the three metals show a wide variety of physical dynamics which affect the ablation properties of each metal. In the early time stages below 50 ps, indicates a decrease in density of the target material. The decrease in reflectivity observed here for Al and stainless steel and is a consequence of the material surface expansion due to stress confinement in the material.

In the intermediate time stages from 100 ps to 1 ns, material motion is observed. Spallation could be temporally and spatially resolved and quantified, and identified as the primary ablation mechanism for bulk Al and stainless steel.

In the final time interval from 2.5 ns to 10 µs the transient reflectivity changes indicate the generation and ejection of particles and clusters until a final state is reached.

For maintaining an optimum energy specific ablation volume the laser ablation should be initiated with a pulse duration shorter than a few ps and afterwards should be left undisturbed by a subsequent pulse until steady state is reached in the µs range, corresponding to a MHz repetition rate.

Acknowledgements

The authors gratefully acknowledge the financial support of this work by the Deutsche Forschungsgemeinschaft (DFG) (grant No. HU 1893/2-1). The authors also acknowledge funding of the Erlangen Graduate School in Advanced Optical Technologies (SAOT) by the DFG in the framework of the German excellence initiative.

References

[1] J. Cheng, C. S. Liu, S. Shang, D. Liu, W. Perrie, G. Dearden, K. Watkins, 2013, A review of ultrafast laser materials micromachining.
[2] K. Sugioka, Y. Cheng, 2014, Ultrafast lasers-reliable tools for advanced materials processing.
[3] C. Momma, B. N. Chichkov, S. Nolte, F. von Alvensleben, A. Tünnermann, H. Welling, B. Wellegehausen, 1996, Short-pulse laser ablation of solid targets, Opt. Commun. 129,p. 134–142.
[4] Y. Nakata, T. Okada, M. Maeda, 2002, Fabrication of dot matrix, comb, and nanowire structures using laser ablation by interfered femtosecond laser beams, Appl. Phys. Lett. 81, p. 4239–4241.
[5] A.-M. Kietzig, S. G. Hatzikiriakos, P. Englezos, 2009, Patterned Superhydrophobic Metallic Surfaces, Langmuir 25, p. 4821–4827.
[6] S. Preuss, A. Demchuk, M. Stuke, 1995, Sub-picosecond UV laser ablation of metals, Appl. Phys. A 61, p.33–37.
[7] M. C. Gower, 2000, Industrial applications of laser micromachining, Opt. Express 7,p. 56.
[8] A. Ancona, F. Röser, K. Rademaker, J. Limpert, S. Nolte, A. Tünnermann, 2008, High speed laser drilling of metals using a high repetition rate, high average power ultrafast fiber CPA system, Opt. Express 16, p. 8958.
[9] P. P. Pronko, S. K. Dutta, J. Squier, J. V. Rudd, D. Du, G. Mourou, 1995, Machining of sub-micron holes using a femtosecond laser at 800 nm, Opt. Commun. 114, p. 106–110.
[10] X. Liu, D. Du, G. Mourou, 1997Laser ablation and micromachining with ultrashort laser pulses, IEEE J. Quantum Electron. 33, p. 1706–1716.
[11] J. Schille, L. Schneider, S. Kraft, L. Hartwig, U. Loeschner, 2016, Experimental study on double-pulse laser ablation of steel upon multiple parallelpolarized ultrashort-pulse irradiations, Appl. Phys. A 122, p. 644.

[12] B. Neuenschwander, B. Jaeggi, M. Schmid, 2013, From fs to Sub-ns: Dependence of the Material Removal Rate on the Pulse Duration for Metals, Phys. Procedia 41, p.794–801.
[13] B. Neuenschwander, B. Jaeggi, M. Schmid, G. Hennig, Surface Structuring with Ultra-short Laser Pulses: Basics, Limitations and Needs for High Throughput, in: Phys. Procedia, volume 56, pp. 1047–1058.
[14] J. Finger, M. Reininghaus, 2014, Eject of pulse to pulse interactions on ultrashort pulse laser drilling of steel with repetition rates up to 10 MHz, Opt. Express 22, p. 18790.
[15] M. Kaganov, I. Lifshitz, L. Tanatarov, 1957, Relaxation between Electrons and the Crystalline Lattice, Sov. Phys. JETP 4, p. 173.
[16] S. I. Anisimov, B. L. Kapeliovich, T. L. Perel-man, 1974, Electron emission from metal surfaces exposed to ultrashort laser pulses, J. Exp. Theor. Phys. 66, p. 375–377.
[17] B. Rethfeld, K. Sokolowski-Tinten, D. von der Linde, S. Anisimov, 2004, Timescales in the response of materials to femtosecond laser excitation, in: Appl. Phys. A, volume 79, pp. 767–769.
[18] X. Shen, Y. P. Timalsina, T.-M. Lu, M. Yamaguchi, 2015, Experimental study of electron-phonon coupling and electron internal thermalization in epitaxially grown ultrathin copper films, Phys. Rev. B 91, p. 45129.
[19] S. S.Wellersho, J. Hohlfeld, J. G¨udde, E. Matthias, 1999, The role of electronphonon coupling in femtosecond laser damage of metals, Appl. Phys. A Mater. Sci. Process, p. 69.
[20] Z. Lin, L. V. Zhigilei, V. Celli, 2008, Electron-phonon coupling and electron heat capacity of metals under conditions of strong electron-phonon nonequilibrium, Phys. Rev. B 77.
[21] D. S. Ivanov, L. V. Zhigilei, 2003, Combined atomistic-continuum modeling of short-pulse laser melting and disintegration of metal films, Phys. Rev. B 68, p. 064114.
[22] E. Leveugle, D. Ivanov, L. Zhigilei, 2004, Photomechanical spallation of molecular and metal targets: molecular dynamics study, Appl. Phys. A 79, 1643–1655
[23] D. Perez, L. J. Lewis, 2003, Molecular-dynamics study of ablation of solids under femtosecond laser pulses, Phys. Rev. B - Condens. Matter Mater. Phys. 67, p. 1–15.
[24] L. V. Zhigilei, Z. Lin, D. S. Ivanov, 2009, Atomistic Modeling of Short Pulse Laser Ablation of Metals: Connections between Melting, Spallation, and Phase Explosion, J. Phys. Chem. C 113, p. 11892–11906.
[25]J. Hohlfeld, S.-S. Wellersho , J. Guedde, U. Conrad, V. Jaehnke, E. Matthias, Electron and lattice dynamics following optical excitation of metals, Chem. Phys. 251 (2000) 237–258.
[26] D. von der Linde, K. Sokolowski-Tinten, 2000, The physical mechanisms of short-pulse laser ablation, Appl. Surf. Sci. 154-155, p.1–10.
[27] K. Sokolowski-Tinten, J. Bialkowski, A. Cavalleri, D. von der Linde, 1998, Observation of a transient insulating phase of metals and semiconductors during short-pulse laser ablation, Appl. Surf. Sci. 127-129, p. 755–760.
[28] I. Carrasco-Garcia, J. M. Vadillo, J. Javier Laserna, 2015, Visualization of surface transformations during laser ablation of solids by femtosecond pump–probe time-resolved microscopy, Spectrochim. Acta Part B At. Spectrosc. 113, p. 30–36.
[29] M. Domke, S. Rapp, M. Schmidt, H. P. Huber, 2012, Ultra-fast movies of thinfilm laser ablation, Appl. Phys. A Mater. Sci. Process. 109, p. 409–420.
[30] S. Rapp, G. Heinrich, M. Domke, H. P. Huber, 2014, The Combination of Direct and Confined Laser Ablation Mechanisms for the Selective Structuring of Thin Silicon Nitride Layers, Phys. Proc. 56, p. 998–1006.
[31] M. Domke, S. Rapp, M. Schmidt, H. P. Huber, 2012, Ultrafast pump-probe microscopy with high temporal dynamic range, Opt. Express 20, p.10330–10338.
[32] J. M. Liu, Simple technique for measurements of pulsed Gaussian-beam spot sizes, 1982, Opt. Lett. 7, p. 196.
[33] M. E. Povarnitsyn, N. E. Andreev, E. M. Apfelbaum, T. E. Itina, K. V. Khishchenko, O. F. Kostenko, P. R. Levashov, M. E. Veysman, 2012, A wide-range model for simulation of pump-probe experiments with metals, Appl. Surf. Sci. 258, p. 9480–9483.
[34] E. Bevillon, R. Stoian, J. P. Colombier, 2018, Nonequilibrium optical properties of transition metals upon ultrafast electron heating, J. Phys. Condens. Matter,p. 30.
[35] J. Schille, L. Schneider, S. Kraft, L. Hartwig, U. Loeschner, 2016, Experimental study on double-pulse laser ablation of steel upon multiple parallelpolarized ultrashort-pulse irradiations, Appl. Phys. A 122, p. 644
[36] A. Semerok, C. Dutouquet, 2006, Ultrashort double pulse laser ablation of metals, Thin Solid Films 453-454. p. 501–505.
[37] D. J. Förster, S. Faas, S. Gröninger, F. Bauer, A. Michalowski, R. Weber, T. Graf, 2018, Shielding effects and re-deposition of material during processing of metals with bursts of ultra-short laser pulses, Appl. Surf. Sci.
[38] T. Kramer, 2017,Increasing the Specific Removal Rate for Ultra Short Pulsed Laser-Micromachining by Using Pulse Bursts, J. Laser Micro/Nanoengineering 12.p. 107–114.T.